

MIT OpenCourseWare  
<http://ocw.mit.edu>

8.13-14 Experimental Physics I & II "Junior Lab"  
Fall 2007 - Spring 2008

For information about citing these materials or our Terms of Use, visit: <http://ocw.mit.edu/terms>.

# 21-cm Radio Astrophysics

MIT Department of Physics

(Dated: March 18, 2008)

Measurement of the Doppler spectrum of interstellar atomic hydrogen and the dynamics of the galactic rotation. A 7.5 foot computer-controlled azimuth-elevation parabolic dish antenna, located on a roof of MIT, is used with a heterodyne measurement chain and digital correlator to observe the Doppler spectrum of the 21-cm hyperfine line of interstellar atomic hydrogen in various directions along the Milky Way. Features of the spiral-arm structure of the Galaxy are deduced from the measured radial velocities of the hydrogen clouds in the galactic disc.

## 1. PREPARATORY PROBLEMS

1. Explain the origin of the 21-cm line of atomic hydrogen.
2. Describe the size and shape of the Galaxy, giving our position from the center in light-years and parsecs (pc). What is the maximum Doppler shift you can expect to observe in the 21-cm line?
3. The parabolic dish antenna used in this experiment has a diameter of 7.5 feet. Suppose it is set so that a source of 21-cm radio emission drifts through its field of view. Plot the signal strength at the output of the diode detector as a function of angle from the center of the field of view.
4. Explain the 21-cm spectrum at  $150^\circ$  and  $60^\circ$  as shown in Figure 7.
5. Explain the signal chain in this experiment (e.g. how the hardware and software serve to convert the signal received by the telescope into a display of signal strength versus frequency).

## 2. PROGRESS CHECK FOR 2ND SESSION

What is the approximate temperature of the sun at 1420 MHz? Plot the power spectrum of galactic hydrogen at 40 degrees galactic longitude and identify all the salient characteristics of the spectrum. Does it agree with Van de Hulst?

## 3. GENERAL STRUCTURE OF THE MILKY WAY

The sun is one among the approximately  $10^{11}$  stars that comprise our Galaxy<sup>1</sup>. From a distant vantage point

this vast array of stars would appear as a rotating spiral galaxy, rather like our famous neighbor galaxy, M31, in the constellation of Andromeda. Detailed examination would reveal a spheroidal component and a concentric disk component. The spheroidal component consists mostly of small ( $M < 0.8M_\odot$ ), old (10-15 billion years) stars (so-called population II) of which most are concentrated in a central “bulge” with a diameter of 3 kpc and the rest are distributed in an extensive “halo” that extends to a radius of 30 kpc or more. The disk component is a thin, flat system of stars, gas and dust  $\sim 200$  pc thick and  $\sim 30$  kpc in radius. The disk stars (called population I) are extremely heterogenous, ranging in age from newborn to the age of the halo stars, and with masses from 0.1 to  $100 M_\odot$ .

The solar system is imbedded in the disk component at a distance of  $8.0 \pm 0.5$  kpc from the center at which radius the circular motion of the Galaxy has a period of approximately  $2 \times 10^8$  years. The naked eye can distinguish about 6,000 of the nearby stars (apparent brightness down to 6 mag) over the entire sky; the myriads of more distant stars of the disk blend into what we perceive as the Milky Way, which is our Galaxy seen edge on.

Between the stars of the disk is the interstellar medium (ISM) of gas and dust comprising approximately 10% of the total mass of the disk. The gas consists primarily of hydrogen and helium with a mass density ratio of 3 to 1 and an average total number density of about  $1 \text{ atom cm}^{-3}$ . The dust is composed mostly of graphite, silicates and other compounds of the light and common elements in microscopic grains containing a small fraction of higher-Z elements, primarily iron. The effect of dust in blocking the light of more distant stars is clearly seen in the “dark lanes” that are conspicuous features of the Milky Way in the region of, e.g., the constellations Cygnus and Aquilla.

The pressure in the ISM is conveniently characterized by the product  $nT$ , where  $n$  is the density in  $\text{atoms cm}^{-3}$  and  $T$  is the temperature in Kelvins. It is roughly constant in the disk and of the order of  $3000 \text{ K cm}^{-3}$ . A wide

---

<sup>1</sup> This description of the Galaxy is a summary of the material contained in Galactic Astronomy by Mihalas and Binney [1], a very useful reference for this experiment. It also contains in Chapter 8 a detailed presentation of the theoretical basis for interpreting the data on galactic kinematics obtained from ob-

---

servations of the Doppler profile of the 21-cm line. Another very nice introduction to the structure of the Milky Way is on-line at <http://cassfos02.ucsd.edu/public/tutorial/MW.html>. Other useful references for this lab are [2–8].

range of observations across the electromagnetic spectrum show that the ISM tends to exist in one of three different states: hot, warm and cool, with temperatures of  $10^6$ ,  $10^4$ , and  $10^2$  K, respectively, and corresponding low, medium and high densities. Within the cool regions there are particularly dense cold regions ( $T \approx 20\text{K}$ ) known as molecular clouds, containing  $\text{H}_2$ , OH, and other more complex molecules. These clouds are the birthplaces of stars that are formed by gravitational contraction of the cloud material. When a burst of star formation occurs in a molecular cloud, the massive stars heat the surrounding ISM to form a warm region of  $10^4$  K. After short lives of a few million years the massive stars explode as supernovas that spew into the ISM portions of the heavy elements that have been synthesized by nuclear fusion in their interiors and by neutron capture during their explosions. The explosions blow “bubbles” of  $10^6$  K gas that merge to form an interconnecting network of hot regions. The hot gas eventually cools and is recycled through molecular clouds in a continuous process that gradually enriches the ISM with the  $Z > 2$  elements of which the Earth and we are composed. Dynamical studies show that there also exists “dark matter” of unknown nature with a mass comparable to or even larger than the total mass of the luminous stars.

An essential key to the development of modern astrophysics was the invention of the spectroscope and its application with photography near the turn of the century to the study of stars and hot nebulae in the visible range of the spectrum. Comparison of stellar spectra with the line spectra of elements in the laboratory yielded information on the composition and temperature of celestial objects, and measurement of wavelength shifts due to the Doppler effect provided determinations of radial velocities which revealed the dynamical properties of systems such as double stars and the general expansion of the universe in the motions of distant galaxies. Most of the interstellar medium, however, is too cold to radiate in the visible part of the spectrum and remained undetectable and its properties largely unknown until fifty years ago. Then, in the midst of World War II, a young Dutch astronomer, H. van de Hulst, examined the theoretical possibilities for detecting cosmic radio waves of some distinct frequency, i.e. a spectral line in the radio portion of the electromagnetic spectrum which would permit measurements of physical conditions and radial motions like those available in the visible spectrum. He predicted that the spin-flip transition of atomic hydrogen would produce such a line at a wavelength near 21 centimeters, and that the unique conditions of low density and temperature in interstellar space are such as to allow time for hydrogen atoms, excited by collision to their hyperfine triplet state ( $F=1$ ), to decay by radiation to the ground state ( $F=0$ ). The line was observed in 1951 by Ewing and Purcell at Harvard, by Christiansen in Sydney, and by Muller and Oort in the Netherlands. Radio observations at 21 cm soon became a major tool of astronomy for exploring and measuring the structure of our

Galaxy and the many distant galaxies accessible to the giant radio telescopes such as the giant single dish antenna at Arecibo in Puerto Rico, the 20-km diameter aperture synthesis array (Very Large Array) in New Mexico, and the transcontinental aperture synthesis array called the VLBA (Very Long Baseline Array).

Atomic hydrogen is the principal constituent of the interstellar medium, and one of the most interesting tracers of galactic structure. Whereas visible light emitted by stars is heavily obscured by interstellar dust, photons with a wavelength of 21 centimeters, emitted in spin-flip transitions of atomic hydrogen in its electronic ground state, reach us from all parts of the Galaxy with little absorption. Measurements of the Doppler shifts of the frequency of the 21-centimeter line determine the radial components (projections onto the line of sight) of motions of the interstellar medium. Analysis of the Doppler shifts in various directions around the galactic plane (i.e. around the Milky Way) reveal the kinematic structure of the galaxy, e.g., the tangential velocity of the matter in the Galaxy as a function of the distance from the center, and, by implication, the geometry of the spiral arms.

## 4. EXPERIMENTAL APPARATUS

### 4.1. Antenna & Motors

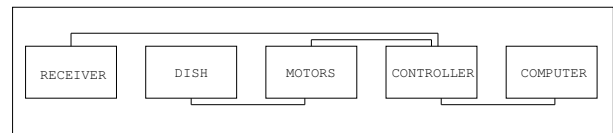


FIG. 1: SRT

The space radio telescope, SRT, is a 7.5 foot diameter parabolic dish antenna manufactured by Kaul-Tronics Inc. and modified by Haystack Observatory<sup>2</sup>. It has a focal length of 85.7cm. It has a beam width of 7.0 degrees (L-band or 1420 MHz)<sup>3</sup>. The dish is mounted on a two-axis azimuth/elevation mount. It is supported by a aluminum frame constructed from C/Ku band mesh that will reflect all incident microwave energy if the surface holes are less than 1/10th of the incident wavelength. The system is controlled using a computer running a java applet that communicates via serial connection with the controller housing a Basic-Stamp microcontroller. The microcontroller in turn controls the motor functions, one drive at a time. A very basic block diagram of the system

<sup>2</sup> Complete specifications for the antenna, mount and receiver are available at [www.haystack.edu/edu/undergrad/srt/index](http://www.haystack.edu/edu/undergrad/srt/index)

<sup>3</sup> The first minimum of the antenna diffraction pattern is given (see any text on optics) by  $1.22 \frac{\lambda}{d} \approx 7^\circ$ .

is shown in Fig. 1. The software calculates galactic coordinate positions from the azimuth-elevation coordinates and a knowledge of the local sidereal time (LST). A brief summary of celestial geometry is provided in Appendix A.

#### 4.2. RECEIVER

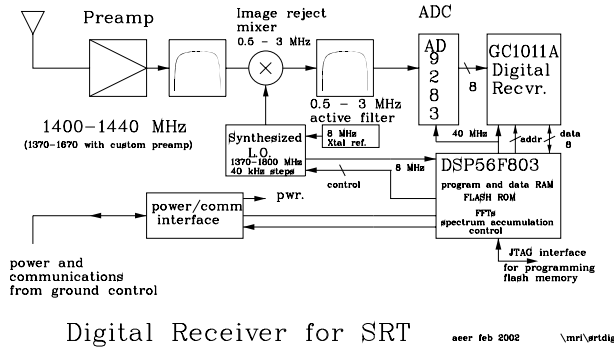


FIG. 2: Receiver

The SRT uses a phasing type single sideband scanning receiver. Fig. 2 shows a block diagram of the radio receiver and subsequent signal processing stages. Radio power arriving from directions close to the axis of the parabolic antenna is focused by reflection to an antenna feed horn. Signals then pass through a band pass filter, low noise pre-amplifier and mixer. The baseband signal is digitized and sent back to the controlling computer over a serial RS-232 link. The central frequency of the synthesized local oscillator (LO) used in the mixer is user selectable from within the JAVA program. This permits the investigator to look at different spectral regions around 1420 MHz.

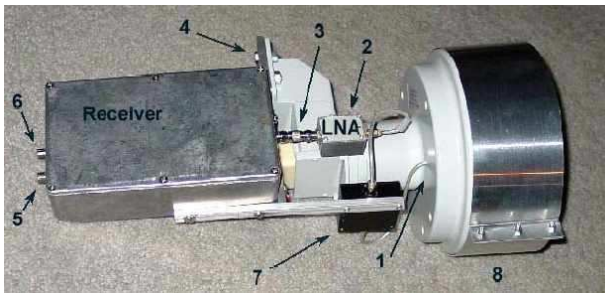


FIG. 3: Feedhorn

- 1 - L-Band probe
- 2 - Low Noise Amplifier
- 3 - Universal Male F to F Coupler
- 4 - Receiver mounting bracket
- 5 - Video Port - Analog signal
- 6 - Power and Communication - Digital Signal
- 7 - Band Pass Filter
- 8 - Feed Horn Extension

Signals pass from the feed horn to the low noise amplifier. The LNA provides a 24dB gain whose output passes through a 40MHz bandpass filter that prevents out of band signals from producing intermodulation in the image rejection mixers. Mixers are circuit elements that form the product of two analog waveforms (in NMR these elements are also called “phase detectors”). It’s two inputs and output are related by the trigonometric relationship:

$$\cos \omega_1 t \cos \omega_2 t = \frac{1}{2} \cos(\omega_1 + \omega_2) + \frac{1}{2} \cos(\omega_1 - \omega_2) \quad (1)$$

Note that both sum and difference frequencies are generated in a mixer. For our application, we band-pass filter the output and throw away the sum frequency contribution. A “balanced” mixer is one in which only the sum and difference frequencies, and not the input signals or their harmonics, are passed, see [http://www.haystack.edu/edu/undergrad/srt/receiver/receiver\\_circuit.html](http://www.haystack.edu/edu/undergrad/srt/receiver/receiver_circuit.html) for more information.

##### 4.2.1. Electronic Noise Calibration

Complete details of the SRT calibration are available at [http://www.haystack.edu/edu/undergrad/srt/receiver/SRT\\_calibration.html](http://www.haystack.edu/edu/undergrad/srt/receiver/SRT_calibration.html). Temperature calibration is performed using a noise diode, whose intensity and spectral distribution is approximately equivalent to a 115 Kelvin blackbody.

The electronic noise calibrator is a diode (Noise/Com NC302L) connected to a small dipole antenna attached to the center of the SRT dish. A small (6mA) current is sent through a controlled bulk avalanche mechanism, resulting in a wide band of frequencies. The dipole emits the signal which is detected by the receiver. To generate the correct wavelength signal, the dipole was fabricated to be 1/2 wavelength, or approximately 10.5 cm. To minimize signal from behind the dipole, the poles are set 1/4 wavelength, or approximately 5.25 cm, above the circular plate at the center of the SRT dish.

Calibration: The software temperature calibration measures the ratio of the received power when the noise diode is turned on and then off again. Both of these power measurements will necessarily contain contributions from spillover and sky. The power ratio is given by

$$\frac{P_{on}}{P_{sky}} = \frac{T_{receiver} + T_{noisecal} + T_{spillover} + T_{sky}}{T_{receiver} + T_{spillover} + T_{sky}} \quad (2)$$

$T_{noisecal}$  is the temperature the electronic noise calibrator radiates and  $P_{on}$  is the power measurement with the calibrator on. The value of  $T_{noisecal}$  was determined by the manufacturer in comparison with an independent vane calibration method.

The figure "Antenna sky noise temperature as a function of frequency and angle from zenith." was removed due to copyright restrictions. Reference: Kraus, John Daniel, and Hsien Ching Ko. Celestial Radiation. Ohio State University, Columbus. Radio Observatory. Report, no. 7. Columbus, Ohio: Ohio State University, 1957.

FIG. 4: Noise Temperature versus angle from zenith. Taken from Kraus, 2nd Edition.

### 4.3. Ground Controller and Software Interface

The ground controller, located in a small aluminum box next to the computer, serves as the interface between the computer and the antenna stepper motors as well as the digital receiver. It uses RS-232 to send commands to the motors and to receive back the digitized spectral temperatures from the receiver.<sup>4</sup> The ground controller should be powered on before the JAVA software is run and turned off again at the end of an experimental session.

The SRT control software interface is a JAVA-based program that runs within the Windows environment. A printed copy of the SRT Manual is located next to the computer. Please do not remove it from the lab!<sup>5</sup>

The SRT software can be run by double-clicking the icon on the windows desktop.

Once the command console has been loaded, the user may access a series of functions via the command toolbar located along the top of the console. Pointing and clicking on any of these buttons will either initiate an automatic sequence response or wait on text input by

the user. Details of the software are in the bound booklet next to the computer (and on the Haystack website). Perhaps the most useful thing to do right away is to begin a log file which will provide you with a continual record of your experiment. To do this, click on the text entry box at the bottom of the Java interface screen and type in the path and filename you wish to log to (e.g. c:\srt\users\username\15aug03.rad). Make sure to create the path first! You can transfer data from this directory to your MIT Server account using Secure FX.

The control program calculates the Local Sidereal and Universal Time based on the computer clock settings within the information sidebar on the right-hand side. **Since Universal Time = Eastern Time + 5 hours (under Standard Time) and = Eastern Time + 4 hours (under Eastern Daylight Savings Time), you much make sure the box "Automatically adjust clock for daylight savings" is checked when setting the computer's clock.** It also indicates the antenna direction in both Equatorial (RA and DEC) and Galactic ('l' and 'b') here. If desired, there is a separate LabVIEW program on the computer's desktop which is a calculator for converting between Horizon and Galactic Coordinate systems.

When turning on the system, pay special attention to any error messages that may appear within the Message Board below the Total Power Chart Recorder. They may indicate that the system has failed to communicate through the coaxial cable (i.e. gnd 0 radio 1). If movement of the dish stops prematurely, "antenna drive status.." or "lost count" may appear in the Motion Status Display Area. If this occurs please turn off the control system (which in turn ends motor power) and have a technical staff member take a look at the motor drive gears. Before powering down the system please return the dish to the stow position.

### 4.4. DATA COLLECTION

The SRT is continually acquiring and processing signals acquired by the dish. The upper right plot shows individual power spectra updated every few seconds. The plot to the left in RED, shows an integrated power spectrum which may be cleared by pressing the "CLEAR" button. It is convenient to check this now by generating a test signal at 1420.4 MHz. This is done by turning on the Marconi RF synthesizer (press the "CARRIER ON/OFF" button and the LED should toggle between ON and OFF). Make sure that you don't leave this synthesizer on except for brief tests and system calibrations.

To deliver a command to the SRT through the JAVA interface, the operator enters text commands into the text box at the bottom of the control console and then clicks the appropriate command button which acts on this data input.

Note that some command button requests must be supplemented with manual command entries. Azimuth and

<sup>4</sup> Full details and schematics of the ground controller are available at <http://www.haystack.edu/undergrad/srt/receiver/schemgndct12.pdf>

<sup>5</sup> The SRT Manual is available online at <http://www.haystack.edu/undergrad/srt/SRTSoftware/SRTManual.pdf>

elevation locations are set using the Horizon Coordinate system. Simply enter the azimuth and elevation in degrees of the position to be observed and the software will check to see if the requested position is currently visible within the mechanical limits of the dish. The control program computes the number of pulses required to turn the telescope and the PC then sends the pulses to the stepping motors. When the telescope reaches the position, if “tracking mode” is on (button text is YELLOW), the PC continues to generate pulses at the rate required to compensate for the earth’s rotation so as to keep the telescope pointing to the specified position in the sky. To turn tracking off, simply click othe button and it should turn RED.

Try the following to get started:

Enter “180 40” in the text window and then press the Azel button. The dish should slowly move to point due south. Press STOW to return the dish to it’s “parked” position at Azimuth=95°,Elevation=4°. Press the “RECORD” button to stop writing to the log file and open it up using a text editor. Think about how you might process such a log file using Matlab’s IMPORT command.

## 5. OBSERVATIONS

You will first test and calibrate the equipment by aligning a noise diode and centering the telescope feed on a peak source, the radio emmission of the Sun. The beamwidth of a radio telescope is the solid-angle measure of the half-power point of the main lobe of the antenna pattern. Measure the half-power beamwidth (HPBW) of the SRT by moving the telescope in a continuous scan across a very bright radio source (e.g. the Sun, Cygnus-X or certain geosynchronous satellites) and plot temperature K vs. degree offset. Measurement of the beam pattern can help the user discover problems with optical alignment or aid in the determination of antenna focus.

Finally, you will observe the power spectrum of the 21-cm hydrogen emission from a sequence of positions along the Milky Way (**identifying which positions is a key task for the student!**). Derive the Galactic rotation curve, and estimate the mass of the Galaxy interior to the circle tangent to the line of sight among your observations that is farthest from the Galactic center. Observe the non-uniformities in the hydrogen distribution revealed by the doppler-induced structures of the line profiles. The multiple-component line profiles are evidence of the spiral-arm structure of the Galaxy.

A list of these and other possible student projects are listed at <http://www.haystack.mit.edu/edu/undergrad/srt/SRT%20Projects/index.html>

### 5.1. The Sun’s Brightness Temperature

To prepare yourself for these measurments, start by reading the Haystack ‘SRT Projects’ page about Solar Observations available on-line through <http://www.haystack.edu/edu/undergrad/srt/index.html>.

Calibrate the system temperature  $T_{sys}$  and set the frequency to “1420.4 4” in order to set the bandwidth as wide as possible to reduce noise variations. To perform a system calibration press the “Cal” button. The noise source is then enabled for approximately 1 second while data is collected . Data is then taken with the noise source off for an additional 1 second. The system software then calculates  $T_{sys}$ , and reports it in the right information sidebar. For the off-source calibration, an area at least two beamwidths (in azimuth, positive or negative) away from the sun is desirable.

There are a couple of different ways to measure  $T_{sun}$ . By clicking on the “npoint” button, a series of measurements surrounding the sun in a 5x5 grid are made with the step size set by the antenna beamwidth defined in the “srt.cat” file. The default value for the beamwidth is 5.0°. The measured power/temperature at each of these grid points is displayed just above the text input box and at the completion of the scan, a 2-D contour plot of the grid is displayed in the graph box at the top of the page. Information about the sweep is then displayed in the information sidebar. The telescope offsets are also adjusted so as to point the dish to the maximum observed signal within the sampled region.

The “npoint” scan is also useful for verifying the targeting accuracy of the system. If the computer clock is set incorrectly or the local latitude and longitude have been inadvertently changed, the sun will NOT appear well centered in this gridded scan. See for example, Figure 5.

The “npoint” scan will focus the dish at the maximum temperature location for the sun when completed. Pointing corrections should be set to the location of peak intensity before continuing the observation session.

To manually specify offsets, enter the offset in the command text area.

```
enter azimuth(degrees) elevation(degrees)
Press ‘‘offset’’ button
```

If you’ve entered something like -5 -5 the effect is that the npoint plot will move right and up.

#### 5.1.1. Alternative $T_{sun}$ measurement

You can also use the “drift” button to cause the dish to be pointed “ahead in time” and then stopped. This will permit the sun, or any other object, to drift through the antenna beam. Recording this data and then plotting the results in Matlab, one can derive an empirical value for the beamwidth of the antenna to compare it

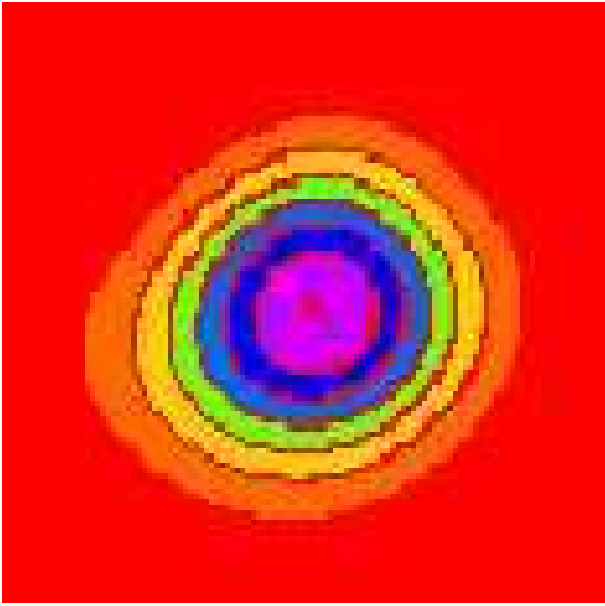


FIG. 5: Typical result from an “npoint” measurement of the Sun’s brightness temperature. The contour plot is generated from a 5x5 series of measurements spaced by 1/2 the antenna beamwidth as specified in the srt.cat text file within the CassiSRT folder on the hard drive.

with the theoretical value. What is the convolution of a finite source with the radiation pattern of the antenna beam? Can you model this? An interesting comparison can be made by comparing your results with the solar flux measured by other antennas around the world.

Measure the power seen by the antenna versus offset to find an estimate for the half-power beam width (HPBW). Your graph should resemble Figure 6.

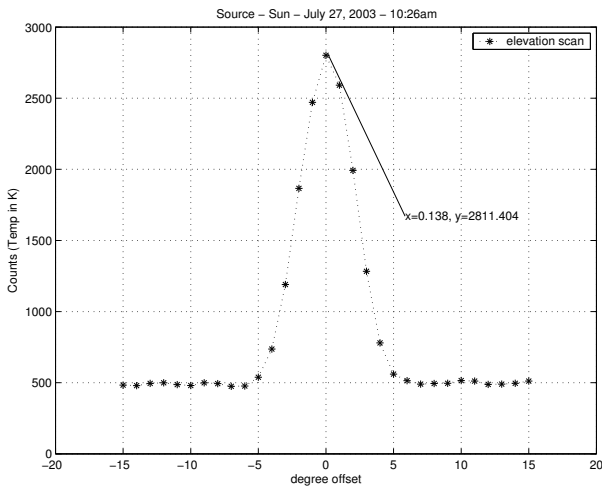


FIG. 6: Sun Scan Elevation

## 5.2. Measuring the Galactic Rotation Curve

To measure the rotation curve of the Milky Way, you will need to record hydrogen line profiles and a known set of galactic coordinates. Your first job is to figure out at which coordinates you will need to point the telescope! Use the software to determine when these regions of the galaxy will be visible from our Northern hemisphere vantage point. Since the visible portion of the galaxy varies with time, you may find it necessary to share observation time with student pairs from other sections.

## 6. ANALYSIS

Compare your plot of the angular response function of the antenna, obtained in the drift scan of the sun, with the theoretical diffraction pattern of a circular aperture. You may need to consult a text on physical optics and use of a computer computation of a Bessel function.

Derive an estimate of the brightness temperature of the sun at 21 cm from your measurements and calibration, taking account of the fraction of the effective solid angle of the antenna response function that is occupied by the sun. Here you may need to study the portion of Shklovski’s book or other reference dealing with brightness temperatures, antenna temperatures and the relation to actual source temperatures.

Reduce the data of your 21-cm line profiles to plots of relative antenna temperature against radial velocity relative to the sun, taking account of the motion of the earth and the antenna around the sun. They should look similar to that obtained in the original Hulst survey shown in Figure 7.

**With the help of the discussions presented in Mihalas and Binney and by Shu, derive from your data a plot of the velocity curve of the Galaxy as a function of radius.** Why are you only able to do so for locations interior to the radial position of our solar system?

### 6.1. Possible Theoretical Topics

1. Hyperfine splitting of the hydrogen ground state.
2. Radiative processes in the sun.
3. Antenna theory.
4. The structure and dynamics of our Galaxy.
5. Radiative transfer.

- 
- [1] D. Mihalas and J. Binney, *Galactic Astronomy* (San Francisco, 1968).
  - [2] F. H. Shu, *The Physical Universe - Chapter 12* (University Science Books, Mill Valley, CA, 1982), this reference gives a clear description of the interpretation of 21cm spectra in terms of the rotation curve of the Galaxy.
  - [3] K. Rohlfs and T. L. Wilson, *Radio Astronomy, 2nd. ed.* (Springer, 1996), a modern handbook of radio astronomy techniques. Section 5.5 describes the relationship between antenna temperature and brightness temperature.<sup>6</sup> Chapter 6 provides a useful discussion of antenna theory.
  - [4] e. a. H. C. van de Hulst, *Bull. of the Astron.*, vol. XII, 117 (Institutes of the Netherlands, 1954).
  - [5] P. Duffett-Smith, *Practical Astronomy With Your Calculator* (Cambridge, 1988), 3rd ed.
  - [6] I. S. Shklovski, *Cosmic Radio Waves* (Cambridge; Harvard University Press, 1960).
  - [7] H. Horowitz and W. Hill, *The Art of Electronics, 2nd Edition* (Cambridge University Press, 1989).
  - [8] F. J. Kerr, *Ann. Rev. Astron. Astroph.* **Vol.7**, 39 (1969).

---

<sup>6</sup> Note, however, the following errors in Section 5.5: The equation between equation (5.59) and equation (5.60) should read  $I_\nu = 2kT/\lambda^2$ . Equation (5.62) should read  $W = \frac{1}{2}A_e \int \int \frac{2kT_b(\theta, \phi)}{\lambda^2} P_n(\theta, \phi) d\Omega$ .

The figure "Survey of hydrogen line profiles at various galactic longitudes"" was removed due to copyright restrictions.  
Reference: van de Hult, H. C., et al. Bulletin of the Astronomical Institutes of the Netherlands, XII, 117, May 14, 1954.  
Amsterdam : North-Holland Pub. Co.

FIG. 7: Survey of hydrogen line profiles at various galactic longitudes. (from H.C. van de Hulst et. al., Bull. of the Astron. Inst. of the Netherlands, XII, 117, May 14, 1954) Note: Pictures are reversed from our images and longitude is given in the old system ( $l^I, b^I$ ).  $l^{II} = l^I + 32.31^\circ$

## APPENDIX A: COORDINATE SYSTEMS

This material is taken in part from Duffett-Smith's book "Practical Astronomy With Your Calculator, 3rd Edition 1988, Cambridge Press". It contains many useful algorithms and is worth checking out of the library or purchasing. There are several coordinate systems which you may meet in astronomy and astrophysical work and here we shall be concerned with four of them: the horizon system (Figure 8), the equatorial system (Figure 10), the ecliptic system (Figure 13) and the galactic system (Figure 9).

**Horizon Coordinates "Az" and "El"** The horizon system, using Azimuth and Altitude (Elevation) is the system under which the SRT is operated.

The figure "Horizon Coordinate System" was removed due to copyright restrictions. Reference: Duffett-Smith, Peter. *Practical Astronomy with Your Calculator*. Cambridge, MA: Cambridge University Press, 1981. ISBN: 9780521284110.

FIG. 8: Diagram of the Horizon coordinate system. Imagine an observer at point 'O'; then her horizon is the circle 'NESW' where North is the direction of the north pole on the Earth's rotation axis and not the magnetic north pole. **Azimuth** increases from 0° (north) through 360°. The **altitude** or **elevation** is 'how far up' in degrees (negative if below the horizon).

**Galactic Coordinates, "l" and "b"** When describing the relations between stars and other celestial objects within our own Galaxy, it is convenient to use the galactic coordinate system. The fundamental plane is the plane of the Galaxy and the fundamental direction is the line joining our Sun to the center of the Galaxy as depicted in Figure 9.

**Equatorial or Celestial Coordinates, "RA" and "DEC"** are the spherical coordinates used to specify the location of a celestial object (Figures 10, 11 and 12). The north celestial pole (NCP) is the direction of the earth's rotation axis, and the celestial equator is the projection onto the sky of the plane of the earth's equator.

**Right ascension (RA)** is the celestial analog of geographic longitude. RA is measured eastward along the celestial equator from the vernal equinox ("V" in Figures 11 and 12) which is the ascending node of the plane defined by the sun's apparent motion (caused by the or-

The figure "Galactic Coordinate System" was removed due to copyright restrictions. Reference: Duffett-Smith, Peter. *Practical Astronomy with Your Calculator*. Cambridge, MA: Cambridge University Press, 1981. ISBN: 9780521284110.

FIG. 9: Diagram of the Galactic coordinate system. The point marked "S" represents the Sun, "G" is the center of the Galaxy and "X" is a star which does not lie in the galactic plane.

bit motion of the earth around the sun) and the celestial equator. In catalogs of celestial objects RA is generally specified in units of hours, minutes and seconds from 0 to 24 hours, but it is often more conveniently specified in degrees from 0° to 360° with a decimal fraction. Declination (DEC) is the celestial analog of geographic latitude. DEC is measured north from the celestial equator along a celestial meridian which is a great circle of constant RA. In catalogs DEC is generally specified in degrees, arc minutes (') and arc seconds ("), but it is also often more conveniently specified in degrees from -90° to +90° with a decimal fraction. (1 hour of RA at constant DEC corresponds to an angle of  $15^\circ \cdot \cos(\text{DEC})$  degrees subtended at the origin).

The **ecliptic** is the intersection of the earth's orbital plane with the celestial sphere. To an observer on earth the sun appears to move relative to the background stars along the ecliptic with an angular velocity of about 1° per day. The angular velocity is not exactly constant due to the eccentricity of the earth's orbit ( $e=0.016722$ ). The period of the earth's orbit is 365.256 days. The **inclination** (ie) of the earth's equator to the ecliptic is 23° 27'. The **ascending node** of the ecliptic with respect to the celestial equator is the intersection of the ecliptic and the celestial equator (the vernal equinox) where the sun in its apparent motion crosses from south to north declinations on March 21. **Precession of the equinoxes** is the motion of the equinoxes along the ecliptic due to precession of the earth's rotational angular momentum about the ecliptic pole. The precession is caused by the torque of the gravitational attractions between the sun and moon and the earth's equatorial bulge. The period of the precession is approximately 25,000 years.

**Ecliptic coordinates** (Figures 14 and 13) are generally used to specify the positions and orientations of objects in the solar system. **Ecliptic longitude** (el) is measured along the ecliptic eastward from the vernal

The figure "Equatorial Coordinate System" was removed due to copyright restrictions. Reference: Duffett-Smith, Peter. *Practical Astronomy with Your Calculator*. Cambridge, MA: Cambridge University Press, 1981. ISBN: 9780521284110.

FIG. 10: Diagram of the Equatorial coordinate system

The figure "Celestial Sphere" was removed due to copyright restrictions. Reference: Duffett-Smith, Peter. *Practical Astronomy with Your Calculator*. Cambridge, MA: Cambridge University Press, 1981. ISBN: 9780521284110

FIG. 12: Diagram of the celestial sphere, showing the celestial north pole (NCP), the celestial equator, the northern ecliptic pole (NEP) and the ecliptic. The points labeled V, S, A, and W are, respectively, the vernal equinox, summer solstice, autumnal equinox, and winter solstice corresponding to the directions of the sun on March 21, June 21, September 21, and December 21. The point labeled "sun" is the direction of the sun on approximately April 21

The figure "Ecliptic Coordinate System" was removed due to copyright restrictions. Reference: Duffett-Smith, Peter. *Practical Astronomy with Your Calculator*. Cambridge, MA: Cambridge University Press, 1981. ISBN: 9780521284110

FIG. 13: Diagram of the Ecliptic coordinate system

rotation of the sun itself, as illustrated in Figure 14, is specified by the ecliptic longitude (ELON) of the ascending node of its equator and the inclination (INCL) of the equator to the ecliptic.

The figure "Celestial Coordinate System" was removed due to copyright restrictions. Reference: Duffett-Smith, Peter. *Practical Astronomy with Your Calculator*. Cambridge, MA: Cambridge University Press, 1981. ISBN: 9780521284110.

FIG. 11: Diagram of the celestial coordinate system

equinox. **Ecliptic latitude** (elat) is measured along a great circle northward from the ecliptic.

The orientation of the orbit of a planet is specified by 1) the ecliptic longitude of the ascending node of the orbital plane and 2) the inclination of the orbit to the ecliptic. Similarly, the orientation of a planet's rotation or the

The figure "showing the relation between the ecliptic and celestial coordinate systems" was removed due to copyright restrictions.  
Reference: Duffett-Smith, Peter. *Practical Astronomy with Your Calculator*. Cambridge, MA: Cambridge University Press, 1981. ISBN: 9780521284110.

FIG. 14: Diagram showing the relation between the ecliptic and celestial coordinate systems

The figure "showing the relations between the quantities involved in setting the position of the telescope about the polar (HA or RA) axis" was removed due to copyright restrictions. Reference: Duffett-Smith, Peter. *Practical Astronomy with Your Calculator*. Cambridge, MA: Cambridge University Press, 1981. ISBN: 9780521284110.

FIG. 15: Diagram of the relations between the quantities involved in setting the position of the telescope about the polar (HA or RA) axis

## APPENDIX B: SIGNAL PROCESSING IN 21-CM RADIO ASTROPHYSICS

For a voltage  $v(t)$  measured in the time domain we can compute the Fourier transform  $V(\nu)$ :

$$V(\nu) = \int v(t)e^{-2\pi i\nu t} dt \quad (\text{B1})$$

Note that  $V(\nu)$  is *complex*, giving us an amplitude and a phase for each frequency component. In our experiment we are not interested in the phase information. Taking the square modulus of the Fourier transform gives us the voltage power spectrum:

$$S(\nu) = [V(\nu)]^2 \quad (\text{B2})$$

$S(\nu)$  is the quantity plotted by the data acquisition software. For the voltage power spectrum, the units are volts<sup>2</sup> (rms), and a sine wave with amplitude  $V_{\text{orms}}$  will produce a signal of amplitude  $V_{\text{orms}}/4$ , which becomes  $V_{\text{orms}}/2$  in the one-sided spectrum that is displayed (see below). The spectrum displayed on the Junior Lab computer screen has units dBm, which is power expressed in dB referred to one milliwatt. The spectrum values are converted to milliwatt units by taking into account the characteristic impedance of the transmission line,  $Z_o = 50 \Omega$ . This is done according to  $\text{dBm} = 10 \log \frac{V_{\text{rms}}^2}{2236^2}$  where the  $50 \Omega$ 's in the numerator and denominator have canceled. The power you measure  $\frac{V_{\text{rms}}^2}{Z_o}$  is the power going down the cable to the A/D converter, related to, but not equal to, the power received at the antenna.

The above expression for the Fourier Transform, refer to a continuous signal measured for an infinite length of time. In practice, instead of  $v(t)$ , we in fact measure  $v_i(t)$ , discrete samples separated by a time interval  $\delta t$ , over a period of time  $\Delta t$ . Thus the number of points measured is  $N = \Delta t/\delta t$ . Our Fourier transform is now the sum

$$V_j(\nu) = \sum_{i=1}^N v_i(t)e^{-2\pi i\nu_j t} \delta t \quad (\text{B3})$$

This differs from the ideal  $V(\nu)$  computed above in some important ways. We have to consider the effects of *sampling* and *windowing*. We also note that the power spectrum has the property of *symmetry about zero frequency*.

**Sampling:** We sample the signal at a rate  $1/\delta t$ , which means that only signals with frequency  $2/\delta t$  or smaller can be reconstructed. In a properly designed spectrometer the sampling range and the *anti-aliasing filter* are chosen with this in mind. This is the reason for the 3 MHz bandpass filter (see Figure 2) and the sampling rate of just over 6 MHz. A strong signal with frequency

larger than 6 MHz that “leaks” through the filter will appear in our power spectrum at an *aliased* frequency with the 0-3 MHz band. Thus, strong interference signals can corrupt your spectra, even though they are outside the bandpass.

Because we use the Fast Fourier Transform (FFT) algorithm to compute the Fourier transform, the spectra are also sampled with values known only at certain values of the frequency. Our frequency “channels” are centered at these values and are separated by

$$\delta\nu = \frac{1}{N\delta t} \quad (\text{B4})$$

**Windowing:** Because the time series is truncated (i.e., we only measure the voltage signal for a finite period of time), the features in the frequency domain are broadened. In other words, a pure harmonic signal, which in principle would appear as a delta function in the frequency domain, in fact appears as a feature with nonzero width. We can express this effect of the limited time span by multiplying by a “window function”  $w(t)$  in the time domain:

$$v_m(t) = w(t)v(t) \quad (\text{B5})$$

For the simplest window function with no weighting,  $w(t)$  is unity during the times of the measurements and zero otherwise:

$$w(t) = 1 \text{ for } -\frac{\Delta t}{2} \leq t \leq \frac{\Delta t}{2} \quad (\text{B6})$$

By the convolution theorem, the Fourier transform of  $v_m(t)$  is the convolution of the Fourier transforms of  $v(t)$  and  $w(t)$ :

$$V_m = W(\nu) * V(\nu) \quad (\text{B7})$$

The Fourier transform of the uniform  $w(t)$  function above is a sinc function in the frequency domain (see Figure 1):

$$W(\nu) = \frac{\sin \pi\nu\Delta t}{\pi\nu} \quad (\text{B8})$$

The width of the sinc function is proportional to  $\Delta t$ . For example, the half width at the first null (HWFN) is  $1/\Delta t$ . Thus, each frequency “spike” in the frequency domain is broadened into a feature shaped like a sinc function with a width determined by the length of the data stream. Note that that the spacing between the nulls is equal to  $1/\Delta t$  and that this is also the channel spacing. The spectral line is also characterized by “sidelobes,” a sort of ringing that can extend far from the main spectral feature. For this choice of window and sampling, the width and sidelobes do not appear in the sampled values of the spectrum if the spectral line is at the center of a channel.

The uniform window is only one possible weighting scheme that can be applied to the data. By changing the weights, we can change the shape of the spectral line

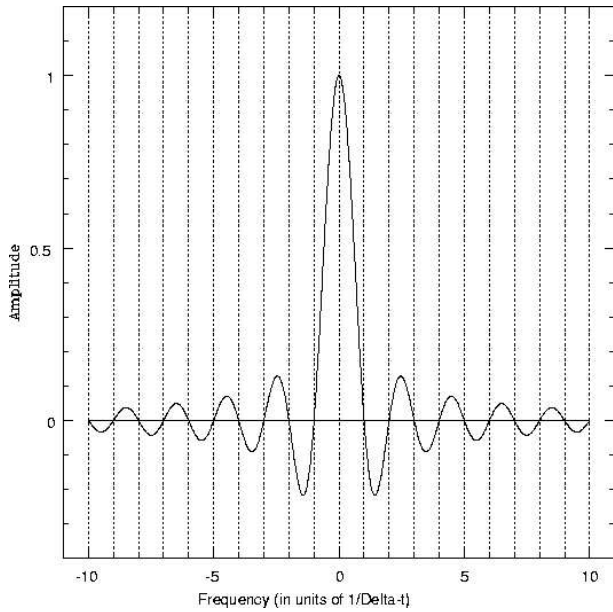


FIG. 16: The Fourier transform of a uniform window of width  $\Delta t$ . The vertical dotted lines show the centers of the frequency channels in the sampled power spectrum, assuming the spectral line is exactly at the center of one channel (which it may not be).

in the frequency domain. The choice should be based on considerations of the expected properties of the spectrum. For example, if we were interested in resolving two closely spaced spectral features, we would choose a weighting scheme that would produce a narrow spectral peak. If we were concerned about interfering signals, it would be prudent to choose a weighting function that produces small sidelobes, even at the cost of a broader spectral peak.

**Symmetry About Zero Frequency** It can be shown that the Fourier transform of a real function is symmetric about zero frequency. For nonzero frequency components, the power is equally divided between  $\pm\nu$ . When we display the spectrum, we just sum the frequency components at  $\pm\nu$  and present a “one-sided” spectrum. Thus, the first frequency bin is at  $\nu = 0$ , and the last frequency bin is at  $\nu = \delta\nu(\frac{N}{2} - 1)$ .

### 1. Fourier Transform Spectroscopy

The radio astrophysics data acquisition program presents you with choices of:

Blocks to average =  $N_{\text{blocks}}$

2 Sided PS bins =  $N_{\text{bins}}$  (corresponds to “n” above)

Window

From these quantities the duty cycle and the frequency channel spacing are computed and displayed.

**Blocks to average** Each “block” of data consists of  $2^{19} = 524288$  samples collected in the time domain

(taking approximately 79msec at a sampling rate of 6.67Msamples/sec). This is the minimum amount of data the program can take. After collecting a block of data, the computer is occupied for some time calculating the power spectrum from  $n\delta t$  segments of the data, applying any user selected windowing function and converting to dBm. A power spectrum is calculated for each block of data, and these spectra are averaged. The fraction of time that the computer is collecting data (as opposed to processing it) is the “duty cycle” that is displayed on the screen. As computers get faster and faster, this duty cycle should approach unity.

**2 Sided PS bins** The signal we measure is real, so the power spectrum we compute is symmetric about zero frequency. The spectrum presented on the PC screen has been “folded” so that the channels at plus and minus the same frequency have been summed. The channel spacing,  $\delta\nu$ , displayed on the screen is

$$\delta\nu = \frac{1}{N_{\text{bins}}\delta t} = \frac{6.67 \text{ MHz}}{N_{\text{bins}}}$$